Journal of Clinical and Translational Research
10.18053/Jctres/08.202206.015

ORIGINAL ARTICLE

Bone marrow mesenchymal stem cell-derived exosomal LINC00847 inhibits the proliferation, migration, and invasion of Ewing sarcoma

Lu Huang[1†], Jiachao Xiong[2†], Jimin Fu[2†], Zhenhai Zhou[2], Honggui Yu[2], Jiang Xu[2], Liang Wu[2], Kai Cao[2*]

1. The Maternal and Children Health Hospital of Jiangxi Province, 318 Bayi Avenue, Nanchang, Jiangxi Province, 330006, China
2. The Orthopedics Hospital, The First Affiliated Hospital of Nanchang University, 1519 Dongyue Avenue, Nanchang County, Nanchang, Jiangxi Province, 330200, China

†These authors contributed equally

*Corresponding author:
Kai Cao
The Orthopedics Hospital, The First Affiliated Hospital of Nanchang University, Nanchang, Jiangxi Province, 330200, PR China.
E-mail: kaichaw@126.com

Article information:
Received: September 22, 2022
Revised: November 7, 2022
Accepted: November 8, 2022

Journal of Clinical and Translational Research
10.18053/Jctres/08.202206.015

Abstract

Background: Ewing sarcoma (ES) is one of the most lethal primary bone tumors with a poor survival rate. Current evidence suggests that extracellular vesicles (EVs) derived from bone marrow mesenchymal stem cells (BMSCs) loaded with abundant biological functional lncRNAs confer therapeutic benefits against the development of various tumors.

Aim: This study aimed to investigate the role of exosomal lncRNAs from BMSCs in the pathogenesis of ES.

Methods: Bioinformatic analysis and qRT-PCR experiments were used to detect the expression level of LINC00847 in ES tissues and cells. Cell biology experiments examined the effect of in vitro proliferation, migration, and invasion abilities and the biological function of BMSCs-derived LINC00847. Finally, we constructed a LINC00847-associated competitive endogenous RNA (ceRNA) network by in silico methods. Gene Set Enrichment Analysis (GSEA) was conducted to reveal the potential molecular mechanism of LINC00847.

Results: We found that LINC00847 was markedly downregulated in ES. Overexpression of LINC00847 inhibited ES cell proliferation, migration, and invasion. Furthermore, BMSCs-derived EVs inhibited the proliferation, migration, and invasion of ES cells by delivering LINC00847. We constructed a LINC00847 related-ceRNA network contains five miRNAs (miR-18a-5p, miR-18b-5p, miR-181a-5p, miR-181c-5p, and miR-485-3p) and four mRNAs (GFPT1, HIF1A, NEDD9, and NOTCH2).

Conclusions: Overall, this study found that BMSCs-EVs-derived exosomal LINC00847 inhibited ES cell proliferation, migration, and invasion. The ceRNA regulatory mechanism of LINC00847 may participate in the pathogenesis of the malignant phenotype of Ewing sarcoma.

Relevance for patients: These findings suggest that BMSCs-derived exosomal lncRNAs may be used for the personalized treatment of tumors, providing a novel theoretical framework for treating ES.

Keywords: Ewing sarcoma, BMSCs, Extracellular vesicles, LINC00847, ceRNA

1. Introduction

Ewing sarcoma is one of the primary malignant bone tumors in children and adolescents with an aggressive phenotype[1]. It can arise anywhere in the body but is typically present at the diaphysis [2]. Approximately 30% of patients with the disease are symptomatic at initial diagnosis and diagnosed with distant metastasis. Metastasis most commonly occurs in the lungs, bone marrow, and bones [3]. About 70-80% of patients with ES survive beyond five years, but the survival rate drops to 30% in patients with metastatic disease[4]. Therefore, it is crucial to understand mechanisms associated with the pathogenesis and progression of ES and identify new biomarkers for early diagnosis and therapy. There is a growing consensus that BMSCs play an essential role in tumor pathogenesis[5,6].

BMSCs, also called bone marrow mesenchymal stem cells, are adult stem cells that reside in the perivascular compartments of bone marrow and are present in many tissues[7]. Current evidence suggests that BMSCs play a significant role in normal biology and some pathological conditions[8]. BMSCs can induce tumor cell proliferation, epithelial-mesenchymal transition (EMT), migration, and metastasis and are significant components of the tumor microenvironment (TME)[5,9]. One recent study found that bi-functional (BF) MSCs expressing TRAIL and truncated anti-GD2 chimeric antigen receptor (GD2 tCAR) harbored features of tumor affinity and tumor-killing in ES[10]. Furthermore, extracellular vesicles (EVs) derived from BMSCs can reportedly carry bioactive substances to regulate tumor progression [11,12]. However, the exact molecular mechanisms of this process remain unclear.

EVs (50-150 nm in diameter) are generated and secreted by cells mediated by a series of regulatory processes[13]. Their cargo determines their functions, which include RNA, DNA, and proteins[14]. In this respect, long noncoding RNAs (lncRNAs) are an extensive class of functional RNAs whose length exceeds 200 nucleotides and function in various cellular processes, including proliferation, migration, invasion, and other tumor biological processes[15]. LncRNAs are abnormally expressed in various cancers serving as prognostic biomarkers and play a critical role in oncogenesis and development[16–18]. An increasing body of evidence suggests that BMSCs-derived exosomal LncRNAs are involved in tumor oncogenesis[11,19–21]. For instance, in hepatocellular carcinoma (HCC), C5orf66-AS1 was

found to be the most significantly upregulated lncRNAs in cancer stem cells (CSCs) after MSCs-derived exosome treatment. Exosomes derived from MSCs inhibit the malignant behavior of HCC-sourced CSCs through the C5orf66-AS1/miR-127-3p/DUSP1/ERK axis[22]. However, the role of BMSC-EVs LncRNAs in ES remains unclear.

The present study focused on the role of BMSCs-EVs in ES and the lncRNAs involved. Using bioinformatics analysis, we constructed a lncRNA-associated ceRNA network that may contribute to malignant behavior in ES. Overall, we revealed the function of BMSCs-EVs in ES and validated the molecules involved using gain and loss-of-function studies.

2. Materials and methods

2.1 Bioinformatic prediction and data processing

Cancer Cell Line Encyclopedia (CCLE) datasets were used to analyze the expression level of LINC00847 in numerous cancers. Genotype-Tissue Expression (GTEx) databases and The Cancer Genome Atlas (TCGA) were used for pan-cancer analysis and downloaded from the TOIL project via the UCSC Xena Browser. Data from public microarrays were obtained from NCBI GEO (National Center for Biotechnology Information Gene Expression Omnibus) and presented in Table S1. LINC00847 expression in ES tissues and cells was studied using GEO datasets (GSE17618, GSE48022, GSE90970). The limma package function "removeBatchEffect" was used to correct batch effects. The packages tidyr, dplyr, and tibble were used for data cleaning, while "ggplot2" was used for data visualization. All data cleaning and visualization were done in R (R software version 4.0.3).

2.2 Survival prognosis analysis

The survival prognosis analysis was performed on 44 ES patients in the GEO dataset (GSE17618). Univariate Cox regression analysis and Kaplan-Meier survival analysis were performed to compare overall survival (OVS) and event-free survival (EFS) between patients with high and low LINC00847 expression. Median values were used as the cutoff values for high and low expression levels of LINC00847. Hazard ratios (HR) with 95% confidence intervals (CI) were estimated with Univariate

Cox regression analysis. P values for K-M survival curves were determined by the log-rank test.

2.3 Cell lines and culture conditions

Human Bone marrow Mesenchymal Stem Cell and Mesenchymal Stem Cell Medium were obtained from Zhong Qiao Xin Zhou Biotechnology Co., Ltd (Shanghai, China). ES cell lines (A673 and SK-N-MC) were stored in our lab. High-glucose Dulbecco's Modified Eagle's Medium (DMEM) was used to culture A673 cells, whereas Minimum Essential Medium (MEM) was used for SK-N-MC cells. Cells were maintained at 37°C with 5% CO_2 and humidified air in both media. Each medium contained 10% FBS, 100 Units/mL penicillin, and 100 µg/mL streptomycin.

2.4 Cell transfection

Small-interfering RNAs (siRNAs) for LINC00847 (Table S2) and LINC00847 overexpression plasmid (pcDNA3.1-LINC00847) were synthesized by HanHeng Biotechnology Co., Ltd (Shanghai, China). The plasmid was constructed using a backbone plasmid containing a CMV promoter encoding a GFP reporter (pcDNA3.1-CMV-GFP). MSCs, A673 cells and SK-N-MC cells were transfected with Lipofectamine® 3000 transfection reagent (Invitrogen, Thermo Fisher Scientific, Inc.) for 48 hours according to manufacturer's protocols and harvested for subsequent assays.

2.5 RNA extraction and gene expression analysis

Subsequently, total RNA (2 µg) was reverse transcribed with an RNA reverse transcription kit (Takara, Dalian, China). Quantitative real-time polymerase chain reaction (qRT-PCR) was used to confirm the expression level of target genes. Primers of LINC00847 and GAPDH are presented in Table S3. Gene expression levels were calculated with the $2^{-\Delta\Delta CT}$ method and standardized by glyceraldehyde-3-phosphate dehydrogenase (GAPDH).

2.6 Cell proliferation assay

Ewing sarcoma A673, SK-N-MC cells were transiently transfected for 24 hours and harvested for cell proliferation assay. The cell proliferation assay was performed using Cell Counting Kit-8 (CCK8,

Dojindo, Shanghai, China) and measured ES cell proliferation according to the manufacturer's protocol. The average of five independent experiments in each group was used to plot the graph.

2.7 Cell migration and invasion assays

After transiently transfected 24 hours, Ewing sarcoma A673, SK-N-MC cells were harvested for cell migration and invasion assays. The cells were suspended using a serum-free medium and diluted to 8 × 10^4/100 µl. In 24-well plates, 100 µl of cell suspension was added to the upper chamber of each chamber (8-µm pore size, Corning), and 700 µl of complete medium containing 20% FBS was added to the lower chamber and further incubated for 48 h. The 24-well plates were removed from the cell incubator, fixed with 4% paraformaldehyde, and stained with 1% crystal violet solution cells. After washing the crystal violet solution, the chamber was cleaned with ultra-pure water, and any non-motile cells were removed from the walls. Finally, cells on the lateral membrane of the chamber were observed under an inverted microscope and photographed. Image J software was used to count and compare the number of cells in each group.

In the cell invasion assay, matrigel gel was diluted with serum-free medium, and the ratio of Matrigel gel to the serum-free medium was 1:4. Subsequently, 50 µl diluted Matrigel gel was added to the upper chamber of the Transwell Chamber. The Matrigel was placed in a cell incubator for 2-3 hours to wait for Matrigel to solidify. Cell suspensions were prepared 24 hours after transfection and counted. The following steps were consistent with the cell migration experiment, in which 1×10^5 cells were added to each chamber.

2.8 Correlation analysis

Pearson correlation coefficients (r) were used to evaluate the transcriptional correlations between the LINC00847 gene and other genes. A p-value < 0.05 indicated a statistically significant correlation.

2.9 Gene set enrichment analysis

Based on the mean expression of LINC00847, differential expression genes (DEGs) were identified

between high- or low- LINC00847 expression patients and ranked by log2 fold change (logFC). To identify signaling pathways regulated by LINC00847, gene set enrichment analysis (GSEA) was conducted using DEGs with ClusterProfiler package[23,24], and hallmark gene sets were obtained from The Broad Institute (https://www.gsea-msigdb.org/gsea/index.jsp). Gene sets with adjusted p.value < 0.05 were regarded as significantly enriched.

2.10 Construction of a competing endogenous RNAs (ceRNA) network

A LINC00847-associated ceRNA network was constructed to reveal the relationship between LINC00847, downregulated miRNAs and upregulated mRNAs, which was visualized in Cytoscape (version 3.9.1; www.cytoscape.org). Briefly, target miRNAs of LINC00847 were predicted using ENCORI (https://starbase.sysu.edu.cn/)[25], RNAInter (http://www.rna-society.org/rnainter/)[26], LncBase (https://diana.e-ce.uth.gr/lncbasev3) databases. The intersection of three target miRNAs predicted datasets were performed to maximize precision. The GSE18546 dataset yielded upregulated differentially expressed miRNAs. Then, the intersection of predicted miRNAs and upregulated miRNAs yielded candidate miRNAs interacting with LINC00847. Based on the miRDB[27], miRTarBase[28], and TargetScan[29,30] databases, the target mRNAs of those miRNAs were predicted. The intersection of three target mRNAs predicted datasets were used to improve the accuracy (Figure S1). Downregulated mRNAs were obtained from GEO microarray dates of MSCs and ES cell lines (GSE17618, GSE48022, GSE90970). Candidate target mRNAs from the three datasets were obtained by the intersection of positively correlated mRNAs of LINC00847, downregulated mRNAs, and targeted mRNA interactions. Finally, a LINC00847-associated ceRNA network was constructed, including LINC00847, candidate miRNAs, and candidate mRNAs.

2.11 Extracellular vesicles extraction and identification

Extracellular vesicle extraction and identification were performed as described previously[1] using ultra-high-speed centrifugation, Western blot analysis, Nanoparticle Tracking Analysis (NTA), and Transmission electron microscopy (TEM). Western blot was used to detect EV markers (TSG101, HSP70, CD63， CD81, and Alix) and negative control (Calnexin). Primary antibodies were purchased

from Proteintech (Wuhan, China).

2.12 Coculture assay of extracellular vesicles and ES cells

The prepared extracellular vesicle suspension (20 μg/ml) was added to the supernatant of the ES cell culture. After 48 hours of coculture, the cells were collected and subjected to cell proliferation, migration, and invasion assays as described previously. The concentration of extracellular vesicles was measured using a BCA kit.

2.13 Statistical analysis

R version 4.03 and GraphPad Prism 9.0 were used for statistical analyses. The data were presented as means ± standard deviations (SD). A student's t-test was used to compare the two groups with normally distributed data. Otherwise, a Chi-square test was used for comparisons between groups. For all comparisons, $p < 0.05$ was regarded as statistically significant.

3. Results

3.1 LINC00847 is downregulated in ES and is associated with a good prognosis

Although CCLE database analysis showed that LINC00847 was downregulated in ES (Figure 1A), the role of LINC00847 in ES remains unclear. Based on the GEO dataset (GSE48022, GSE90970, GSE17618), we found that LINC00847 was downregulated in ES tissues (Figure 1B) and cells (Figure 1C), compared to BM-MSCs. These results were corroborated by qRT-PCR, which demonstrated significant downregulation of LINC00847 in A673 and SK-N-MC cells (Figure 1 D). Using univariate Cox proportional analysis and Kaplan-Meier survival curves, the expression level of LINC00847 was confirmed as a prognostic factor. Specifically, ES patients with low expression of LINC00847 exhibited good overall survival (Hazard ratio = 0.19, 95% CI:0.08-0.45, p = 0.003, Figure 1E) and event-free survival (Hazard ratio = 0.16, 95% CI:0.07-0.4, p = 0.002, Figure 1F) rates. Taken together, our results suggest that a low expression level of LINC00847 correlated with a good prognosis in ES patients.

3.2 LINC00847 inhibits ES cell proliferation and mobility

To investigate the biological function of LINC00847 in ES cells, LINC00847 was transiently overexpressed in A673 cells and SK-N-MC cells (via PCDNA3.1-LINC00847 plasmid) (Figure 2A). These A673 and SK-N-MC cells were used for subsequent experiments. Subsequently, ES cell proliferation was detected by CCK-8 assays. Compared to the control group, LINC00847 upregulation resulted in an attenuated proliferation of A673 and SK-N-MC cells (Figure 2B, C). Likewise, the invasion and migration capability of ES cells (A673 and SK-N-MC) were diminished after LINC00847 overexpression. (Figure 2D E). Overall, LINC00847 could inhibit ES cell proliferation, migration, and invasion.

3.3 BMSC-derived EVs deliver LINC00847 and inhibit the proliferation, migration, and invasion of ES cells

The patterns of LINC00847 expression were examined in BMSC-EVs. Validation of the isolation and purification of EVs was carried out using TEM, NTA, and western blot analysis. The obtained EVs were of the expected shape and size under TEM (Figure 3A). According to NTA, the average extracellular vesicle size was 134.7 nm for 98.5 percent of all participants (Figure 3B). EV markers (HSP70, TSG-101, Alix, CD81, and CD63) and an endoplasmic reticulum marker (calnexin, negative control of EVs) were detected by western blot (Figure 3C). A qRT-PCR analysis showed upregulation of LINC00847 in BMSCs-EVs when LINC00847 was overexpressed in BMSCs. On the other hand, knocking down LINC00847 in BMSCs inhibited its expression in extracellular vesicles (Figure 3D E). Furthermore, ES cells cocultured with LINC00847-rich BMSCs-EVs exhibited higher LINC00847 expression levels, as determined by qRT-PCR (Figure 3F). Following coculture with PKH-26 labeled BMSCs-EVs, ES cells exhibited red fluorescence, suggesting that ES cells internalized the EVs (Figure 3G). In a nutshell, these results suggested that LINC00847 could modulate tumor oncogenesis and progression via the EVs.

Additionally, ES cells cultured with LINC00847-rich BMSCs-EVs exhibited lower proliferation ability (Figure 4A B), consistent with the migration and invasion assays. After co-culture with LINC00847-rich BMSCs-EVs for 48 hours, ES cell proliferation, migration, and invasion ability were significantly suppressed(Figure 4C D). These findings indicate that BMSCs-EVs LINC00847 inhibit ES cell

proliferation, migration, and invasion.

3.4 The ceRNA regulatory network of LINC00847 in ES

According to previous findings, lncRNA function is related to its subcellular location. Using the lncLocator[31] (http://www.csbio.sjtu.edu.cn/bioinf/lncLocator) and LnCeCell[32] (http://bio-bigdata.hrbmu.edu.cn/LnCeCell), we found that LINC00847 was localized in the cytoplasm, extracellular vesicles, and nucleus (Figure 5A B). LncBase, ENCORI, and RNAInter databases were used to predict target miRNAs for LINC00847. The intersection of the three gene sets yielded 16 common target miRNAs (Figure 5C). Incorporating the intersection of predicted miRNAs and upregulated miRNAs (from the GSE18546 dataset), five potential ceRNA-miRNAs were obtained (Figure 5D), which included miR-18a-5p, miR-18b-5p, miR-181a-5p, miR-181c-5p, and miR-485-3p. MiRDB, miRTarBase, and Targetscan databases were used to predict the target mRNAs of 5 ceRNA-miRNAs. BM-MSCs and ES cell lines microarray data (from GSE17618, GSE48022, GSE90970) were used to detect downregulated mRNAs (logFC < -1, adjust.p.value < 0.05). Positively correlated mRNAs of LINC00847 in ES cell lines were identified in the CCLE database. Based on the intersection of these gene sets (predict target mRNAs, downregulated mRNAs, LINC00847 positively correlated mRNAs), 37 potential ceRNA-mRNAs were identified (Figure 5E). Finally, a ceRNA network containing LINC00847, five miRNAs, and 37 mRNAs (Figure 5 F) was constructed, revealing the potential mechanism of LINC00847 action.

3.5 GSEA screening of the molecular mechanism of LINC00847

Based on the mean expression of LINC00847, differential expression genes were implemented between high- or low- LINC00847 expression patients and performed for GSEA. GSEA results of the two GEO datasets are presented in Figure 6A and 6B, respectively. Six downregulated hallmark geneset were found by incorporating the intersection of the two GSEA results (Figure 6 C). It included E2F TARGETS, G2M CHECKPOINT, GLYCOLYSIS, MITOTIC SPINDLE, MITOTIC SPINDLE, and MYOGENESIS (Figure 6 D). Then, mRNAs from the ceRNA network were mapped to gene sets from GSEA. Four genes were critical to the significantly enriched hallmark genesets (Figure 6 E). Specifically,

HIF1A and NOTCH2 were the core genes of the G2M CHECKPOINT geneset. GFPT1 was the core gene of the GLYCOLYSIS geneset. NEDD9 and NOTCH2 were the core genes of the MITOTIC SPINDLE geneset. Accordingly, we postulated that LINC00847 might affect the expression of these four crucial genes by sponging miRNAs and consequently modulating the malignant phenotype of ES.

3.6 Pan-cancer analysis of the correlation between LINC00847 and ceRNA-mRNAs

We obtained four core mRNAs belonging to the ceRNA network in our previous analysis. Furthermore, pan-cancer correlation analysis was performed to identify the relationship between LINC00847 and four critical mRNAs. The expression of LINC00847 was evaluated by analyzing TCGA and GTEx databases (Figure 7A). Then, the correlation of LINC00847 with four ceRNA-mRNAs (GFPT1, HIF1A, NEDD9, and NOTCH2) was demonstrated in cancer samples (Figure 7B), normal tissues (Figure 7C), based on the data from The Cancer Genome Atlas (TCGA), Genotype-Tissue Expression (GTEx) databases, respectively. The results indicated that LINC00847 showed a positive correlation in expression level with the four core genes (GFPT1, HIF1A, NEDD9, and NOTCH2) in most cancer and tissues. Overall, these results demonstrated that aberrant expression of LINC00847 might regulate the expressions of four mRNA (GFPT1, HIF1A, NEDD9, and NOTCH2) to modulate ES malignant processes by sponging five miRNAs (that was, miR-18a-5p, miR-18b-5p, miR-181a-5p, miR-181c-5p, and miR-485-3p).

4. DISCUSSION

ES is a malignant bone tumor commonly observed in children and adolescents[33]. LncRNAs have long been regarded as potential targets for the treatment of ES[17]. In the present study, we found that BMSCs-EVs-derived LINC00847 could inhibit ES cell proliferation, migration, and invasion. We then inspected the molecular mechanisms of LINC00847, screened by bioinformatics analysis. The LINC00847 related-ceRNA network comprising five miRNAs (miR-18a-5p, miR-18b-5p, miR-181a-5p, miR-181c-5p, and miR-485-3p) and four mRNAs (GFPT1, HIF1A, NEDD9, and NOTCH2) was constructed and regulated the malignant phenotype of Ewing sarcoma.

We first uncovered that LINC00847 was aberrantly downregulated in ES cells and tissues. Subsequently,

LINC00847 gain-of-function experiments identified the tumor-suppressive role of LINC00847 in ES cells. However, the function of LINC00847 in tumors has been largely understudied. One study revealed that LINC00847 served as a tumor promoter during hepatocellular carcinoma progression by acting as a sponge of miR-99a to induce E2F2 expression[34]. In addition, LINC00847 could decoy miR-181a-5p and upregulate ZEB2, promoting the proliferation, cell cycle progression, migration, and invasion of laryngeal squamous cell carcinoma (LSCC) cells[35]. Meanwhile, another study provided compelling evidence that upregulation of LINC00847 accelerated the progression of non-small Cell Lung Cancer (NSCLC) by modulating the miR-147a/IFITM1 axis[36]. Based on the literature, the present study demonstrated that LINC00847 functions differently in different tumor types. Furthermore, overexpression of LINC00847 may be a therapeutic approach for ES.

MSC-EVs exhibit various biological characteristics, including but not limited to pro-regenerative and anti-inflammatory properties[37]. As an alternative to MSCs, MSC-EVs possess several advantages, such as a safer quality, lower immunogenicity, and the ability to cross biological barriers. It avoids potential complications induced by MSCs, such as ectopic tumor formation, contamination, and immune rejection[38]. The above findings demonstrate that MSC-EVs could be an effective therapy. In the present study, BMSCs-EVs containing LINC00847 inhibited ES cell proliferation, migration, and invasion. These findings suggest that BMSCs-EVs may be used for the personalized treatment of tumors. Nonetheless, further research is warranted on BMSCs-EVs in clinical settings. Specifically, several crucial issues need to be resolved, including production methods, given that current methods for EV production exhibit low efficiency, limiting EV development in preclinical and clinical studies[39]. The five main isolation methods are differential ultracentrifugation, density gradient ultracentrifugation, size exclusion centrifugation, precipitation, and immune-based capture [40]. It is not feasible to isolate EVs in large enough quantities for clinical use with currently available technology. Furthermore, it is critical to figure out the biodistribution and targeting mechanisms of BMSCs-EVs.

The molecular mechanisms underlying the therapeutic effects of BMSCs-EVs derived LINC00847 remain largely unclear in ES. A study reported that lncRNA C5orf66-AS1 was upregulated in cancer

stem cells of hepatocellular carcinoma after BMSCs-EVs treatment. C5orf66-AS1 could upregulate DUSP1 expression by sponging microRNA-127-3p and reduce the proliferation, migration, invasion, proangiogenesis, and self-renewal abilities of HCC-CSCs[22]. Moreover, BMSCs-EVs could promote osteosarcoma proliferation, migration, and invasion via delivering lncRNA PVT1 into osteosarcoma cells. Mechanistically, PVT1 upregulated the expression of ERG by sponging miR-183-5p[41]. These results substantiated that BMSCs-EVs derived lncRNA might play a ceRNA function in the regulation of tumorigenesis. Accordingly, we constructed a LINC00847-associated-ceRNA network, which revealed that dysregulation of LINC00847 expression might regulate the levels of four mRNAs (GFPT1, HIF1A, NEDD9, and NOTCH2) to inhibit ES malignant processes by sponging five miRNAs (miR-18a-5p, miR-18b-5p, miR-181a-5p, miR-181c-5p, and miR-485-3p). However, further experimental verification is needed.

In conclusion, LINC00847 is an excellent prognostic factor of ES and acts as a tumor suppressor inhibiting cell proliferation, migration, and invasion. BMSCs-derived EVs inhibit ES cell proliferation, migration, and invasion by delivering LINC00847. We established a LINC00847 related-ceRNA network comprising five miRNAs (miR-18a-5p, miR-18b-5p, miR-181a-5p, miR-181c-5p, and miR-485-3p) and four mRNAs (GFPT1, HIF1A, NEDD9, and NOTCH2) which may regulate the malignant phenotype of Ewing sarcoma.

Acknowledgements

This study was supported by the Key Project of the Natural Science Foundation of Jiangxi Provincial (No. 20202ACB206004), the National Natural Science Foundation of China (No. 81860473), Major Discipline Academic and Technical Leaders Training Program of Jiangxi Province (No. 20204BCJ22026).

Conflicts of Interest

The authors have declared no conflicts of interest.

References

1. Xiong J, Wu L, Huang L, Wu C, Liu Z, Deng W, Ma S, Zhou Z, Yu H, Cao K. Lncrna foxp4-as1 promotes progression of ewing sarcoma and is associated with immune infiltrates. Front Oncol 2021;11:718876.

2. Xu J, Zhang Z, Huang L, Xiong J, Zhou Z, Yu H, Wu L, Liu Z, Cao K. Let-7a suppresses ewing sarcoma cscs' malignant phenotype via forming a positive feedback circuit with stat3 and lin28. J Bone Oncol 2021;31:100406.

3. Riggi N, Suva ML, Stamenkovic I. Ewing's sarcoma. N Engl J Med 2021;384:154-164.

4. Grunewald TGP, Cidre-Aranaz F, Surdez D, Tomazou EM, de Alava E, Kovar H, Sorensen PH, Delattre O, Dirksen U. Ewing sarcoma. Nat Rev Dis Primers 2018;4:5.

5. Liang W, Chen X, Zhang S, Fang J, Chen M, Xu Y, Chen X. Mesenchymal stem cells as a double-edged sword in tumor growth: Focusing on msc-derived cytokines. Cell Mol Biol Lett 2021;26:3.

6. Montazersaheb S, Fathi E, Mamandi A, Farahzadi R, Heidari HR. Mesenchymal stem cells and cancer stem cells: An overview of tumor- mesenchymal stem cell interaction for therapeutic interventions. Curr Drug Targets 2022;23:60-71.

7. Pittenger MF, Discher DE, Peault BM, Phinney DG, Hare JM, Caplan AI. Mesenchymal stem cell perspective: Cell biology to clinical progress. NPJ Regen Med 2019;4:22.

8. Jafari A, Rezaei-Tavirani M, Farhadihosseinabadi B, Zali H, Niknejad H. Human amniotic mesenchymal stem cells to promote/suppress cancer: Two sides of the same coin. Stem Cell Res Ther 2021;12:126.

9. Aravindhan S, Ejam SS, Lafta MH, Markov A, Yumashev AV, Ahmadi M. Mesenchymal stem cells and cancer therapy: Insights into targeting the tumour vasculature. Cancer Cell Int 2021;21.

10. Golinelli G, Grisendi G, Dall'Ora M, Casari G, Spano C, Talami R, Banchelli F, Prapa M, Chiavelli C, Rossignoli F, Candini O, D'Amico R, Nasi M, Cossarizza A, Casarini L, Dominici M. Anti-gd2 car mscs against metastatic ewing's sarcoma. Transl Oncol 2022;15:101240.

11. Zhang F, Guo J, Zhang Z, Qian Y, Wang G, Duan M, Zhao H, Yang Z, Jiang X. Mesenchymal stem cell-derived exosome: A tumor regulator and carrier for targeted tumor therapy. Cancer Lett 2022;526:29-40.

12. Shojaei S, Hashemi SM, Ghanbarian H, Salehi M, Mohammadi-Yeganeh S. Effect of mesenchymal stem cells-derived exosomes on tumor microenvironment: Tumor progression versus tumor suppression. J Cell Physiol 2019;234:3394-3409.

13. Gandham S, Su X, Wood J, Nocera AL, Alli SC, Milane L, Zimmerman A, Amiji M, Ivanov AR. Technologies and standardization in research on extracellular vesicles. Trends Biotechnol 2020;38:1066-1098.

14. Moller A, Lobb RJ. The evolving translational potential of small extracellular vesicles in cancer. Nat Rev Cancer 2020;20:697-709.

15. Kazimierczyk M, Kasprowicz MK, Kasprzyk ME, Wrzesinski J. Human long noncoding rna interactome: Detection, characterization and function. Int J Mol Sci 2020;21.

16. Adnane S, Marino A, Leucci E. Lncrnas in human cancers: Signal from noise. Trends Cell Biol 2022;32:565-573.

17. Liu SJ, Dang HX, Lim DA, Feng FY, Maher CA. Long noncoding rnas in cancer metastasis. Nat Rev Cancer 2021;21:446-460.

18. Wang J, Zhang X, Chen W, Hu X, Li J, Liu C. Regulatory roles of long noncoding rnas implicated in cancer hallmarks. Int J Cancer 2020;146:906-916.

19. Zhang WL, Liu Y, Jiang J, Tang YJ, Tang YL, Liang XH. Extracellular vesicle long non-coding rna-mediated crosstalk in the tumor microenvironment: Tiny molecules, huge roles. Cancer Sci 2020;111:2726-2735.

20. Pathania AS, Challagundla KB. Exosomal long non-coding rnas: Emerging players in the tumor microenvironment. Mol Ther Nucleic Acids 2021;23:1371-1383.

21. Da M, Jiang H, Xie Y, Jin W, Han S. The biological roles of exosomal long non-coding rnas in cancers. Onco Targets Ther 2021;14:271-287.

22. Gu H, Yan C, Wan H, Wu L, Liu J, Zhu Z, Gao D. Mesenchymal stem cell-derived exosomes block malignant behaviors of hepatocellular carcinoma stem cells through a lncrna c5orf66-as1/microrna-127-3p/dusp1/erk axis. Hum Cell 2021;34:1812-1829.

23. Subramanian A, Tamayo P, Mootha VK, Mukherjee S, Ebert BL, Gillette MA, Paulovich A, Pomeroy SL, Golub TR, Lander ES, Mesirov JP. Gene set enrichment analysis: A knowledge-based approach for interpreting genome-wide expression profiles. Proc Natl Acad Sci U S A 2005;102:15545-15550.

24. Yu G, Wang L-G, Han Y, He Q-Y. Clusterprofiler: An r package for comparing biological themes among gene clusters. Omics : a journal of integrative biology 2012;16:284-287.

25. Li JH, Liu S, Zhou H, Qu LH, Yang JH. Starbase v2.0: Decoding mirna-cerna, mirna-ncrna and protein-rna interaction networks from large-scale clip-seq data. Nucleic Acids Res 2014;42:D92-97.

26. Kang J, Tang Q, He J, Li L, Yang N, Yu S, Wang M, Zhang Y, Lin J, Cui T, Hu Y, Tan P, Cheng J, Zheng H, Wang D, Su X, Chen W, Huang Y. Rnainter v4.0: Rna interactome repository with redefined confidence scoring system and improved accessibility. Nucleic Acids Res 2022;50:D326-D332.

27. Chen Y, Wang X. Mirdb: An online database for prediction of functional microrna targets. Nucleic Acids Res 2020;48:D127-D131.

28. Huang HY, Lin YC, Cui S, Huang Y, Tang Y, Xu J, Bao J, Li Y, Wen J, Zuo H, Wang W, Li J, Ni J, Ruan Y, Li L, Chen Y, Xie Y, Zhu Z, Cai X, Chen X, Yao L, Chen Y, Luo Y, LuXu S, Luo M, Chiu CM, Ma K, Zhu L, Cheng GJ, Bai C, Chiang YC, Wang L, Wei F, Lee TY, Huang HD. Mirtarbase update 2022: An informative resource for experimentally validated mirna-target interactions. Nucleic Acids Res 2022;50:D222-D230.

29. Agarwal V, Bell GW, Nam JW, Bartel DP. Predicting effective microrna target sites in mammalian mrnas. ElIF-e 2015;4

30. McGeary SE, Lin KS, Shi CY, Pham TM, Bisaria N, Kelley GM, Bartel DP. The biochemical basis of microrna targeting efficacy. Science 2019;366.

31. Cao Z, Pan X, Yang Y, Huang Y, Shen HB. The lnclocator: A subcellular localization predictor for long non-coding rnas based on a stacked ensemble classifier. Bioinformatics 2018;34:2185-2194.

32. Wang P, Guo Q, Hao Y, Liu Q, Gao Y, Zhi H, Li X, Shang S, Guo S, Zhang Y, Ning S, Li X. Lncecell: A comprehensive database of predicted lncrna-associated cerna networks at single-cell resolution. Nucleic Acids Res 2021;49:D125-D133.

33. Hesla AC, Papakonstantinou A, Tsagkozis P. Current status of management and outcome for patients with ewing sarcoma. Cancers (Basel) 2021;13.

34. Tu LR, Li W, Liu J, Song XG, Xu HW. Lncrna linc00847 contributes to hepatocellular carcinoma progression by acting as a sponge of mir-99a to induce e2f2 expression. J Biol Regul Homeost Agents 2020;34:2195-2203.

35. Li W, Hu X, Huang X. Long intergenic non-protein coding rna 847 promotes laryngeal squamous cell carcinoma progression through the microrna-181a-5p/zinc finger e-box binding homeobox 2 axis. Bioengineered 2022;13:9987-10000.

36. Li H, Chen YK, Wan Q, Shi AQ, Wang M, He P, Tang LX. Long non-coding rna linc00847 induced by e2f1 accelerates non-small cell lung cancer progression through targeting mir-147a/ifitm1 axis. Front Med (Lausanne) 2021;8:663558.

37. Gowen A, Shahjin F, Chand S, Odegaard KE, Yelamanchili SV. Mesenchymal stem cell-derived extracellular vesicles: Challenges in clinical applications. Front Cell Dev Biol 2020;8:149.

38. Joo HS, Suh JH, Lee HJ, Bang ES, Lee JM. Current knowledge and future perspectives on mesenchymal stem cell-derived exosomes as a new therapeutic agent. Int J Mol Sci 2020;21.

39. Whitford W, Guterstam P. Exosome manufacturing status. Future Med Chem 2019;11:1225-1236.

40. Thery C, Witwer KW, Aikawa E, Alcaraz MJ, Anderson JD, Andriantsitohaina R, et al. Minimal information for studies of extracellular vesicles 2018 (misev2018): A position statement of the international society for extracellular vesicles and update of the misev2014 guidelines. J Extracell Vesicles 2018;7:1535750.

41 Zhao W, Qin P, Zhang D, Cui X, Gao J, Yu Z, Chai Y, Wang J, Li J. Long non-coding rna pvt1 encapsulated in bone marrow mesenchymal stem cell-derived exosomes promotes osteosarcoma growth and metastasis by stabilizing erg and sponging mir-183-5p. Aging (Albany NY) 2019;11:9581-9596.

Figures

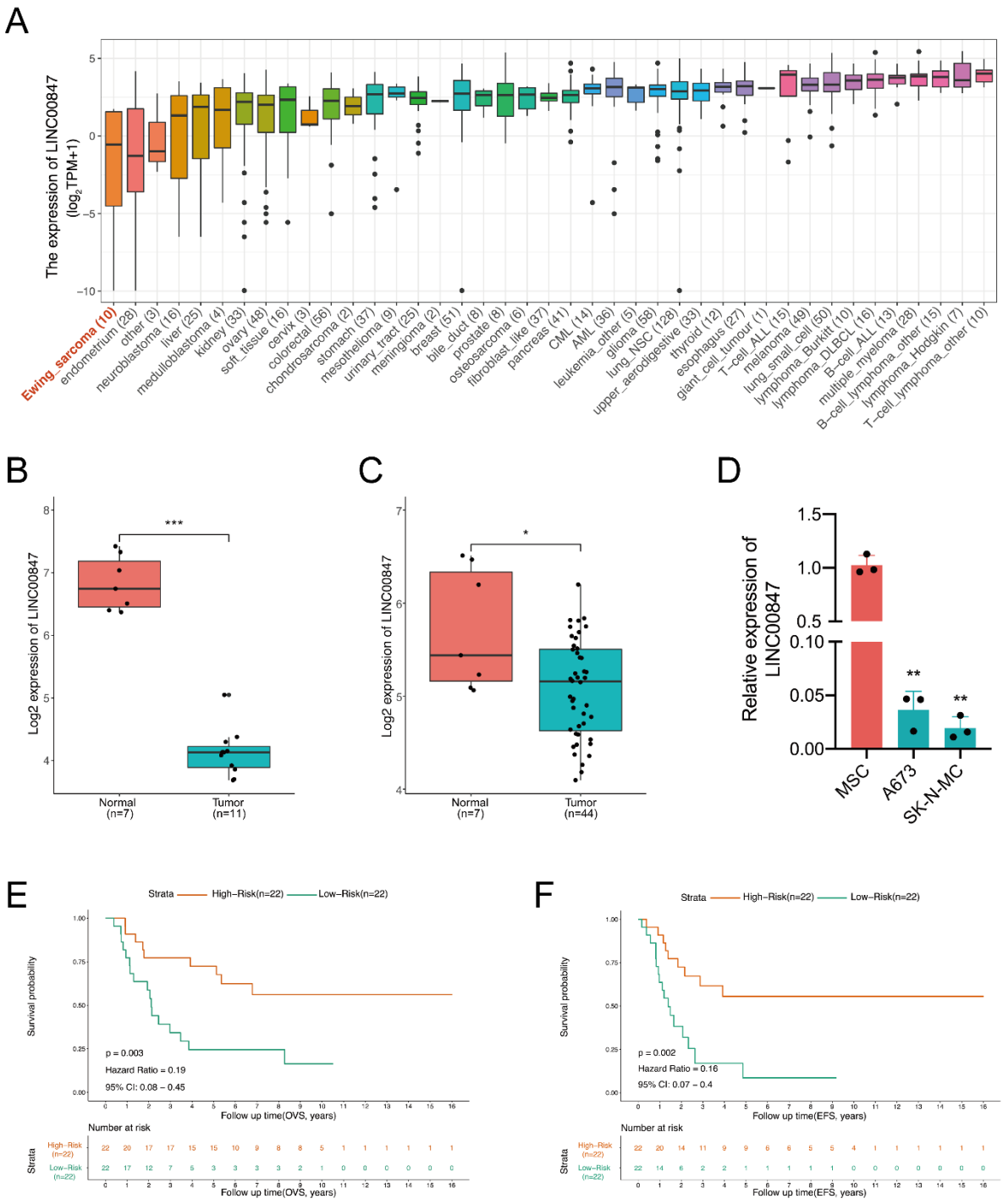

Figure 1. LINC00847 expression profile in ES and association with good prognosis. A. The expression levels of LINC00847 in datasets from the CCLE database. B and C. The expression levels of LINC00847 in ES tissues and cells from the GEO database, compared with BMSCs. D. The expression levels of LINC00847 in ES cell lines A673 and SK-N-MC detected via qRT-PCR. E and F, During survival analysis and univariate Cox regression analysis of ES patients, LINC00847 expression was associated

with overall survival (OS) and event-free survival (EFS). * $p < 0.05$, ** $p < 0.01$, *** $p < 0.001$.

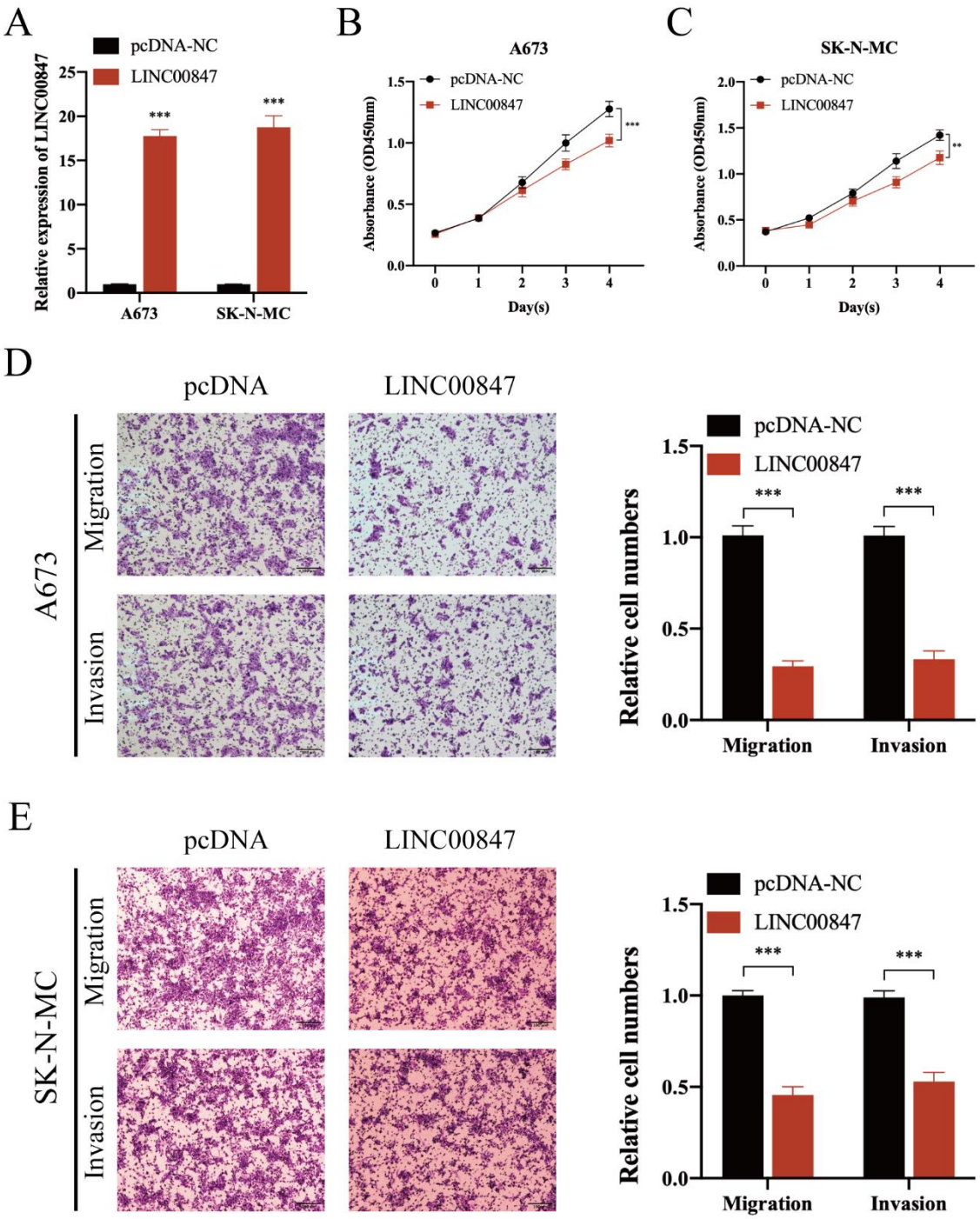

Figure 2. The overexpression of LINC00847 enhanced the proliferation, migration, and invasion abilities of ES cells. A. The LINC00847 overexpression plasmid was transiently transfected into ES cells, and gene expression was detected by qRT-PCR. B and C. In the CCK-8 assay, LINC00847 overexpression inhibited ES cell proliferation. D and E. Overexpression of LINC00847 inhibited cell

migration and invasion in ES. * p < 0.05, ** p < 0.01, *** p < 0.001.

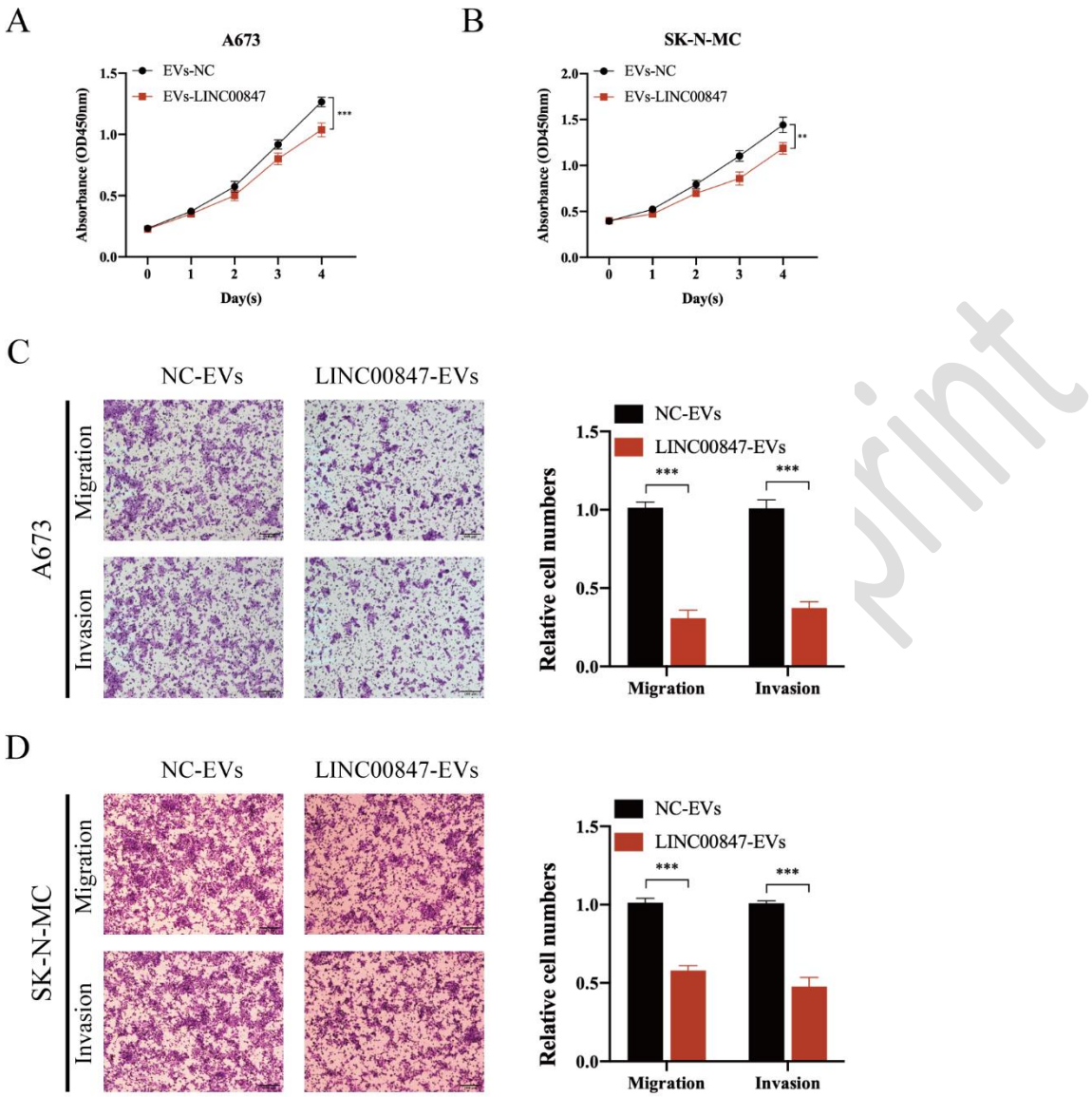

Figure 3. BMSC-derived EVs deliver LINC00847 to ES cells. A. Transmission electron microscopy (TEM) was used to determine the morphology of extracellular vesicles. B. Nanoparticle Tracking Analysis (NTA) was used to measure the particle size of extracellular vesicles. C. The western blotting assay was used to detect the protein levels of extracellular vesicle markers. D. The expression of LINC00847 was measured following up- or downregulation of LINC00847 in BMSCs by qRT-PCR. E. Following up- or downregulation of LINC00847 in BMSCs, qRT-PCR was used to detect LINC00847 expression in BMSCs-EVs. F. ES cells cocultured with LINC00847-rich BMSCs-EVs showed higher LINC00847 expression levels using qRT-PCR. G. Immunofluorescence examined PKH-26 labeled BMSCs-EVs (red fluorescence) uptaken by ES cells (blue fluorescence). ** p < 0.01, *** p < 0.001.

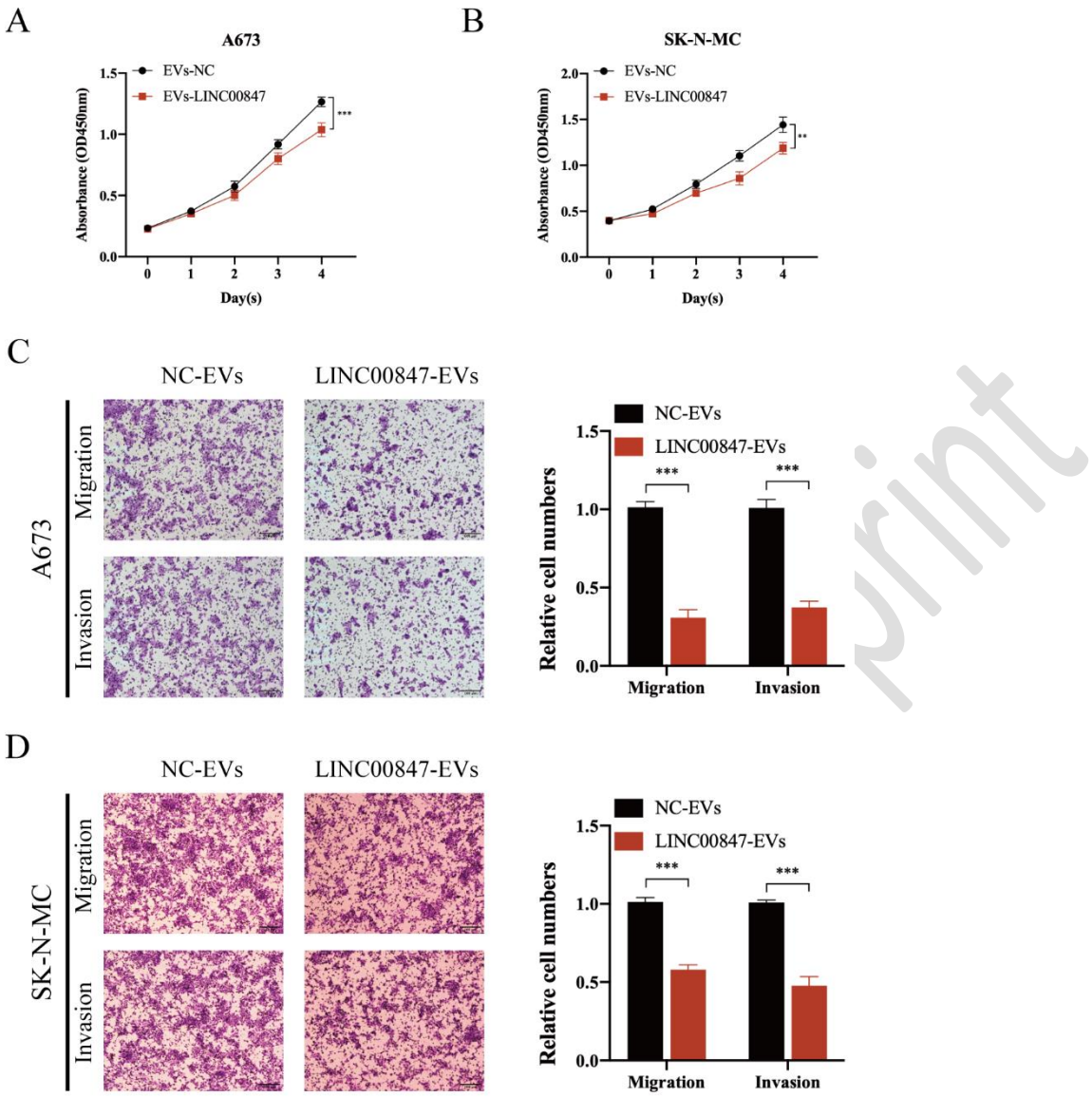

Figure 4. BMSCs-EVs LINC00847 significantly inhibited the proliferation, migration, and invasion of ES cells. A and B. The proliferation ability of ES cells cultured by LINC00847-rich BMSCs-EVs was determined by CCK8 assay. C and D. Transwell assays evaluated the changes in the migration and invasion of ES cells cultured by LINC00847-rich BMSCs-EVs.

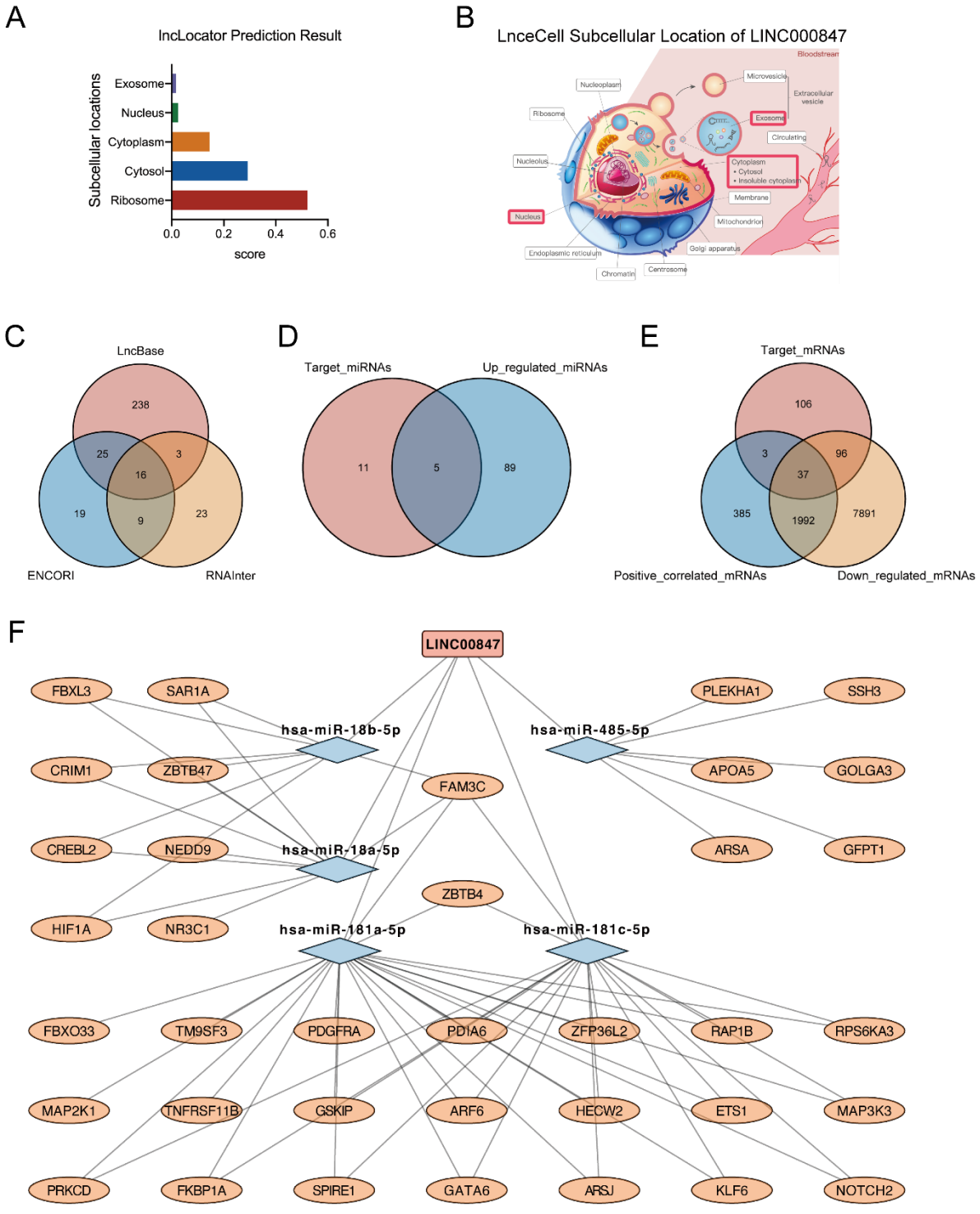

Figure 5. A ceRNA regulatory network for LINC00847 was constructed in ES. A and B. LncLocator and LnceCell predicted the subcellular localization of LINC00847. C. LncBase, ENCORI, and RNAInter database were used to predict target miRNAs for LINC00847. Based on the intersection of these gene sets, 16 common target miRNAs were obtained. D. Combining predicted miRNAs with those upregulated in ES, the final five miRNAs were included in the ceRNA network. E. MiRDB, miRTarBase,

and Targetscan databases were used to predict the target mRNAs of 5 ceRNA-miRNAs. ES microarray data was used to detect down-regulated mRNAs (logFC < -1, adjust.p.value < 0.05). Positively correlated mRNAs of LINC00847 were discovered in the CCLE database. As a result, 37 potential ceRNA-mRNAs based on the intersection of these gene sets were generated (predict target mRNAs, downregulated mRNAs, LINC00847 positively correlated genes). F. Cytoscape was used to visualize the ceRNA network.

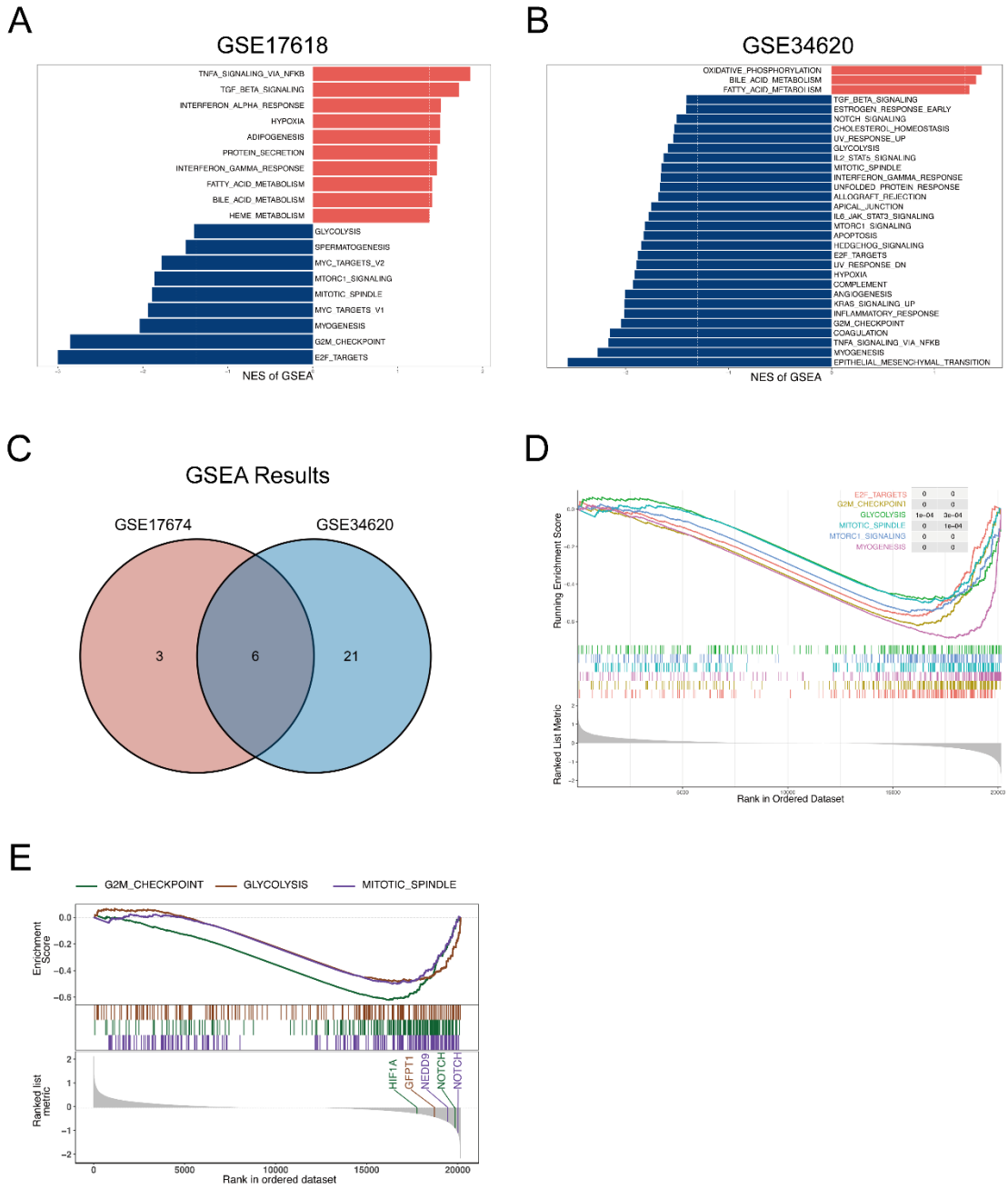

Figure 6. The molecular mechanism of LINC00847 was determined from GSEA analysis. A and B. Genes were arranged using fold-change values and underwent GSEA. C and D. Combining the GSEA results of two GEO datasets, six commonly downregulated hallmarks genesets were finally identified. E. The GSEA identified four crucial ceRNA-mRNAs associated with three downregulated hallmarks genesets in the ceRNA network.

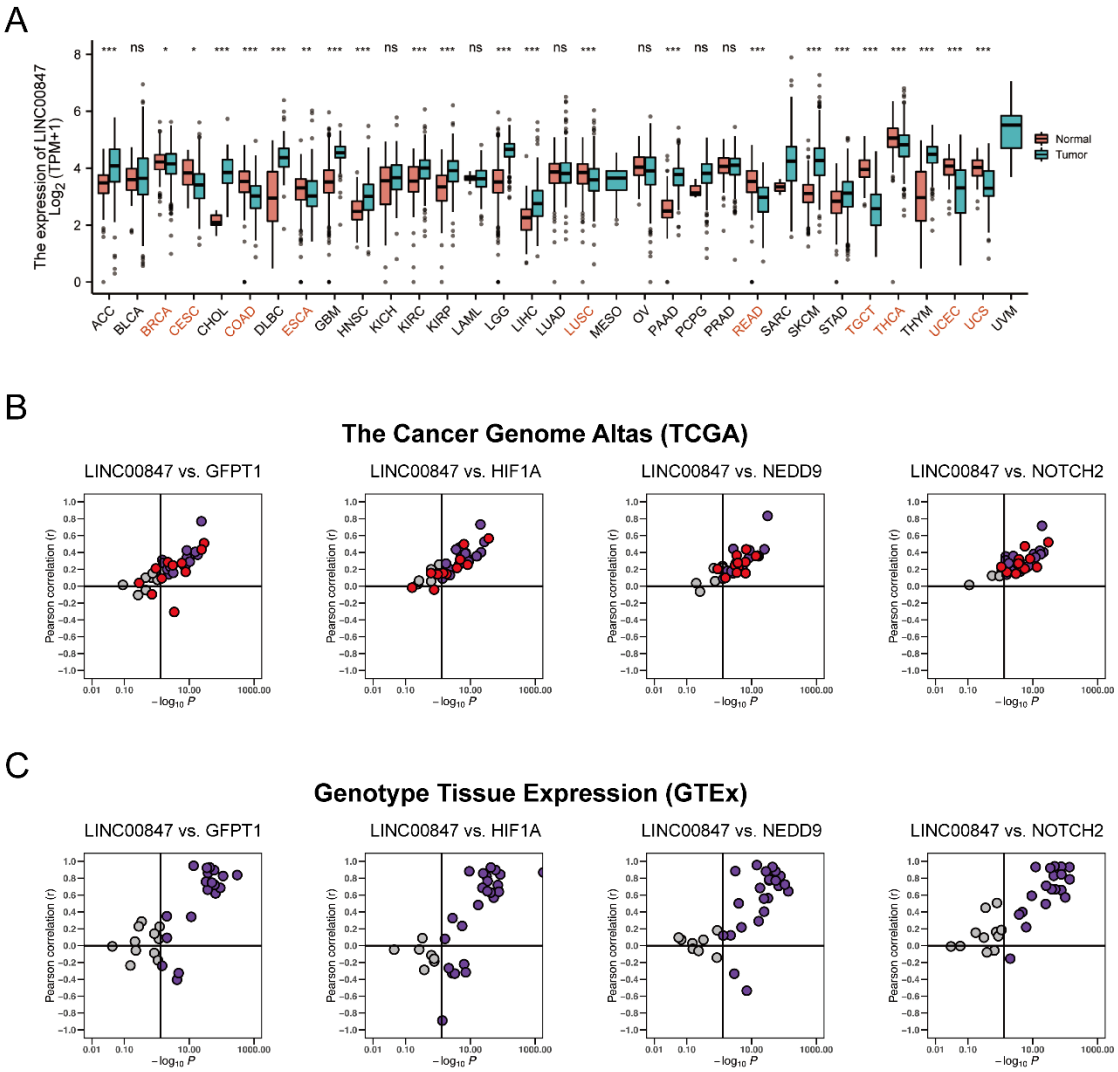

Figure 7. Pan-cancer analysis of the correlation between LINC00847 and ceRNA-mRNAs. A. The LINC00847 expression levels were detected using the TCGA and GTEx datasets. Red variables on the x-axis indicated that the expression levels of LINC00847 were reduced. B and C. Correlation of LINC00847 with four ceRNA-mRNAs (that was, GFPT1, HIF1A, NEDD9, and NOTCH2) in expression in cancer samples (B), normal tissues (C), based on the data from The Cancer Genome Atlas (TCGA), Genotype-Tissue Expression (GTEx), respectively. * $p < 0.05$, ** $p < 0.01$, *** $p < 0.001$.